A Hybrid Image Enhancement Algorithm for Effective Concrete Surface Crack Classification

*Sheerin Sitara Noor Mohamed[1] & Kavitha Srinivasan[2]

[1]*Research Scholar, Department of Computer Science and Engineering, Sri Sivasubramaniya Nadar College of Engineering Kalavakkam, Tamil Nadu, India*
[2]*Assosiate Professor, Department of Computer Science and Engineering, Sri Sivasubramaniya Nadar College of Engineering Kalavakkam, Tamil Nadu, India*

[1]*sheerinsitaran@ssn.edu.in;* [2]*kavithas@ssn.edu.in*

Abstract: *Huge number of images are acquired and analysed every day for a range of applications in civil infrastructure. One such application is the identification of cracks in concrete surface images, which is a challenge owing to their low contrast and resolution, blurriness, noise and information loss. Existing image enhancement algorithms improve either contrast or resolution to a rather limited extent. This paper proposes a Hybrid Image Enhancement (HIE) algorithm to improve both the contrast and resolution of concrete surface images using the Wavelet transform and Singular Value Decomposition (SVM). The enhanced concrete surface crack images are classified into specific crack types. The classification comprises preprocessing, crack detection, feature extraction and crack classification. The images are initially preprocessed using the Wiener filter to remove blurriness, following which cracks are detected using morphological operations and discontinuities in the segmented crack regions eliminated using the K-Dimensional Tree algorithm. Features are extracted from the segmented regions using statistical and geometric features. The image is classified thereafter into specific crack types using algorithms from three different neural network, kernel and tree based categories. The proposed HIE algorithm is validated using quantitative metrics and the results obtained are compared with those from State-of-the-Art methods and datasets. The results have shown that the HIE algorithm offers significantly improved accuracy of between 6% and 10% in the classification of concrete surface images.*

Keywords*:* Concrete surface images, Singular Value Decomposition, Hybrid Image Enhancement, K-Dimensional Tree, Types of cracks

1. Introduction

A crack is a complete or incomplete separation of a region into two or more parts, created through aging, breaking or fracturing. Cracks are broadly classified into two categories, regular and irregular. Regular cracks include the longitudinal [1], transverse [2], thin [3], sealed [4], tiny [5] and large [5], while miscellaneous [1], complex [6] and mixed [7] constitute irregular cracks. Cracks arise across different concrete, sheet metal,

* Corresponding author

alloy steel and asphalt surfaces. Of these, cracks on concrete surfaces commonly occur in buildings, bridges, roads and pavements, given the wear and tear associated with daily life. In addition, concrete surfaces are used in civil infrastructure construction like foundations, staircases and slabs because of their durability, fire resistance and cost effectiveness.

A crack in a concrete surface is indicative of degradation in the structure over a period of time, culminating in severe environmental damage and calling for periodic maintenance. Real time issues arising from the presence of cracks have included, in recent times, increased road accidents[1], building collapses[2] and the closure of bridges[3] spanning across rivers. The occurrence of such events in real time suggests a need for the regular maintenance of concrete surfaces and rectification of cracks at the earliest. In general, cracks are manually checked by civil infrastructure inspectors. There are, however, issues with such checks, including the relatively small number of human experts in the field, inadequate domain knowledge, the time and expense entailed in inspection as well as the risk to life involved in the careful examination of damaged structures. To address these issues, an automatic crack detection and classification method evolved over a period, even though many real time issues or challenges are not resolved.

This paper addresses a key issue related to the automatic crack detection and classification of low contrast and high resolution images of cracked concrete. A Hybrid Image Enhancement (HIE) algorithm is proposed to overcome existing drawbacks and improve the accuracy and reliability of the image classification system for concrete cracks. In addition, the proposed algorithm is suitable for concrete images with multiple cracks, acquired through the use of Unmanned Aerial Vehicles (UAV), robots and low quality sensor cameras.

The rest of this paper is organized as follows: Section 2 discusses the background to preprocessing, image processing and machine learning in the crack detection domain. The proposed system is explained with algorithms in the next section. Section 3 explains the proposed system with algorithms. Section 4 describes the dataset and analyzes the experimental results using quantitative metrics for the three datasets used. Section 5 concludes the paper with future work.

2. Related Work

Research on crack detection and classification methods began to emerge from 2002 onwards. Methods that analyze images of concrete cracks in different surfaces incorporate preprocessing, enhancement, segmentation and classification of crack types. Popular and widely used preprocessing techniques for cracked concrete images are the Savitzky-Golay [8] and Wiener filters [2]. The Savitzky-Golay filter increases the signal-to-noise ratio without distorting the image, while the Wiener filter method has fewer computations and better noise resistance. A review of image enhancement algorithms used in the literature on cracked concrete images in different surfaces show a preference for the Canny edge [2], Laplace operator and histogram equalization [9], threshold approach [10], Wavelet transform [2], [11], and Singular Value Decomposition (SVD) [12]. [2] applied the Canny edge detection algorithm to extract structural information from images and dramatically reduce the quantum of data to be processed. [9] suggested that the Laplace operator and

[1] https://www.gilmanbedigian.com/accidents-caused-by-poor-road-quality-and-conditions-in-dc/

[2] https://www.thehindu.com/news/cities/Delhi/ashok-vihar-building-collapse-accused-ignored-cracks/article25063214.ece

[3] https://metro.co.uk/2020/08/13/major-london-bridge-closed-immediate-effect-heatwave-causes-cracks-13125914/

histogram equalization methods reduce noise and enhance image contrast. [10] applied the thresholding approach for enhanced contrast in concrete surface images prior to detecting regions with cracks. [11] applied the statistical characteristics of the wavelet coefficient in different frequency bands to maximize the resolution of road surface images. [12] applied the SVD on low contrast asphalt surface images to enhance them prior to detecting regions with prominent cracks. [13] proposed a hybrid method (a combination of the min-max gray level discrimination, Otsu method and shape analysis algorithm) to identify crack defects with better accuracy by boosting the contrast of building surface images. It is inferred from these studies that there is no single algorithm which improves contrast and resolution simultaneously for concrete surface images. Therefore, a HIE algorithm using a combination of the Discrete Wavelet Transform (DWT) and SVD is proposed to refine the contrast and resolution of concrete surface images before classifying crack types. [14] suggested the same combination in their review of concrete surface image classification approaches. Further, it is observed that the combined DWT and SVD approach works just as well on medical images by enhancing the brightness of CT scan images [15].

Crack regions are identified, following which the region of interest is segmented using crack detection techniques such as least square binarization [16], Otsu method, integrated algorithm [17] and gradient method [18]. The crack region is identified and the region of interest segmented using maximum entropy [16], Histogram of Oriented Gradients (HOG) [19], morphological operations [2, 17, 20 - 21]. Maximum entropy and least square binarization are combined to sustain the uniform grey values within each block using block wise binarization. The HOG method reduces the influence of illumination information and identifies cracked regions by capturing silhouettes and contour information. The Otsu method performs automatic image thresholding to distinguish the foreground from the background, based on the single intensity value. A morphological operation processes the image based on shapes, using dilation, erosion and reconstruction approaches. This particular method is chosen in this research, since the boundary regions are correctly identified and the pattern of the crack is retrieved.

From the segmented crack region, significant features are extracted for crack classification. The different features extracted include the mean, standard deviation, area, eccentricity, length, width, correlation, rectangularity length, aspect ratio length, intensity and histogram [1-2, 17, 21]. However, [22] proved that while a large number of significant features offers higher accuracy, the computational time is likely to increase, based on the application.

The extracted features are used to classify cracks into specific longitudinal, transverse, crocodile and non-crack types, using supervised algorithms like the Support Vector Machine (SVM), Multi-Layer Perceptron (MLP), AdaBoost, random forest, and decision tree [2, 10, 21, 24 - 25]. Of these, the SVM is ideally suited to small sample sets because of its strong generalization ability which requires that the number of dimensions be greater than the number of samples for effectiveness [2]. [21] suggested that the MLP obtains rapid prediction for large datasets owing to its feed forward design, even though it takes longer time for training. [5] found that the AdaBoost is flexible enough to be combined with other machine learning algorithms to enhance performance, though the dataset has noisy data and outliers. A study by [24] found that the random forest is robust to noise and most suitable for large datasets with a minimum possibility of overfitting. [23] suggested that the decision tree is suited to both classification and regression problems because it accepts incomplete data and supports numerical and categorical features. [25] suggested that the decision tree heuristic algorithm, which combines the C4.5 and J48, is preferable for multi-crack classification. The dataset used in this paper is considered for validating the proposed HIE algorithm using machine learning techniques.

Development in technology and computations using a Graphics Processing Unit (GPU) have facilitated the introduction of Deep Neural Network (DNN) frameworks for image classification. The DNN techniques applied in crack image classification include Convolutional Neural Networks (CNN) and transfer learning approaches using pre-trained models. [26] compared the CNN with the SVM and boosting method for binary crack classification, resulting in 89%, 73% and 74% accuracy, respectively. Also, the dataset used

in [26] is considered for validating the proposed HIE algorithm using machine learning techniques. Further, [27] suggested that the enhanced crack images improved their performance by 1% to 12% with the CNN and pre-trained VGG16, VGG19 and Inception ResNet models. Images without enhancement, on the contrary, showed little improvement, thus justifying the importance of enhancement algorithms for crack images.
From the study of existing work on crack detection and classification, appropriate methods are chosen and modified for the preprocessing, enhancement, segmentation and classification of the crack region. Also, a hybrid approach is proposed to overcome issues with low resolution and contrast through enhancement.

3. System Design

The design of the proposed system, using the HIE algorithm for the effective crack classification of low resolution and low contrast images, is shown in Figure 1. The model comprises two stages: (i) Crack detection and connection, and (ii) Feature extraction and crack classification.

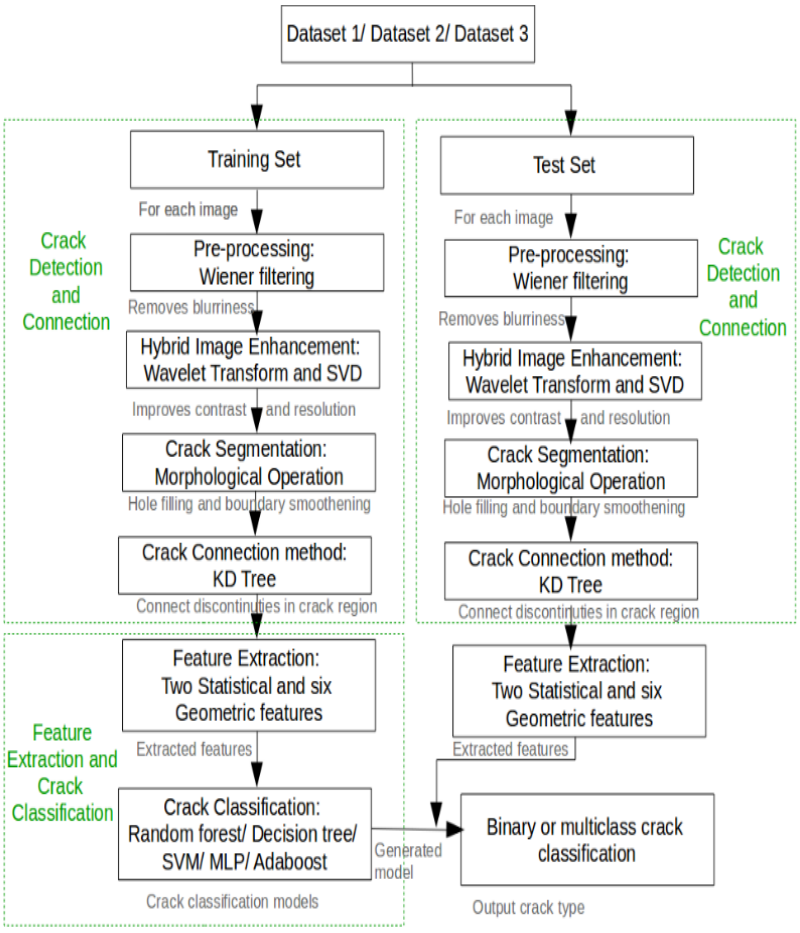

Figure 1. Proposed system for crack detection and classification

3.1. Crack Detection and Connection

3.1.1 Preprocessing - Wiener filter: The Wiener filter is used in preprocessing to eliminate blurriness in the image. It also reduces the mean square error by maintaining the tradeoff between noise smoothening and inverse filtering. In addition, information on tiny cracks is preserved for accurate classification and the process described in Algorithm 1.

Algorithm: Wiener filter

Input: 2D concrete surface image with noise (I_{in})

Output: Noise removed image (B_{out})

procedure **Wiener Filter** *(I_{in})*

- Procedure to remove the blurriness in the concrete crack image
- Z, the number of samples

for k ⟶ 1 to Z do

Read the image matrix I_k

for i ⟶ 1 to M do

for j ⟶ 1 to N do

Compute mean for the input image $I_k(i,j)$ as follows

$$\mu = \frac{1}{MxN}\sum_{(i,j)\varepsilon S} I_k(i,j) \quad (1)$$

where S denotes the MxN neighbourhood of each pixel (i,j)

Compute variance for the input image $I_k(i,j)$ from the mean value

$$\sigma^2 = \frac{1}{MxN}\sum_{(i,j)\varepsilon S}({I_k}^2(i,j) - \mu^2) \quad (2)$$

Generate blurriness removed image from computed mean and variance

$$B_{out} = \mu + \frac{\sigma^2 - v^2}{\sigma^2}(I_k(i,j) - \mu) \quad (3)$$

where v^2(noise variance)[35] is the average of all the estimated local variance

end for

end for

end for

return B_{out}

end procedure

3.1.2 Hybrid Image Enhancement (HIE) – Wavelet transform and SVD: The proposed HIE algorithm is a combination of the Wavelet transform and SVD methods. Wavelet transformation, which is applied to consolidate information on cracks in the lower approximation sub band, is further enhanced using the SVD. This is because SVD, enhances the crack target by eliminating the noise inference and improving the resolution with contrast. The proposed HIE is described in Algorithm 2 and the workflow shown in Figure 2. The DWT, EHL, ELH, EHH, ELL and IDWT in Figure 2 stand for the Discrete Wavelet Transform, Estimated High Low, Estimated Low High, Estimated High High, Estimated Low Low, and Inverse Discrete Wavelet Transform, respectively. The HIE algorithm works in 3 stages: resolution enhancement (Function 1), contrast enhancement (Function 2) and reconstruction of the enhanced image in phases (Function 3).

Algorithm: Hybrid Image Enhancement

Input: Noise removed image with low resolution and poor contrast (I_{in})
Output: Enhanced image (E_{out})
procedure *Hybrid Image Enhancement* (I_{in})

- Procedure to improve the contrast and resolution of concrete crack image
- N, the number of samples

for i ⟶ 1 to N do
(E_{LH}, E_{HL}, E_{HH}) ⟶ REP (I_{in})
LL_{SVD} ⟶ CEP (I_{in})
E_{out} ⟶ RCEIP (LL_{SVD}, E_{LH}, E_{HL}, E_{HH})
end for
end procedure

Function: Resolution Enhancement Phase

Input: Noise removed image with low resolution and poor contrast (I_{in})
Output: Enhanced high frequency sub-bands (E_{LH}, E_{HL}, E_{HH})
function *REP* (I_{in})

- Function to enhance high frequency components

Read the image matrix I_{in}
for all points in I_{in} do
Compute four sub-bands from I_{in} using DWT as follows

$$LL(x,y) = \phi(x)\phi(y) \quad (4)$$
$$LH(x,y) = \psi(x)\phi(y) \quad (5)$$
$$HL(x,y) = \phi(x)\,\psi(y) \quad (6)$$
$$HH(x,y) = \psi(x)\,\psi(y) \quad (7)$$
$$\phi_{j,k}(x) = 2^{j/2}\,\phi(2^j x - k) \quad (8)$$
$$\psi_{j,k}(x) = 2^{j/2}\,\psi(2^j x - k) \quad (9)$$

where $\phi(x), \phi(y), \psi(x)$ *and* $\psi(y)$ are functions of discrete variables.
Compute difference image from I_{in} and LL sub-band

$$d(x,y) = |I_{in}(x,y) - LL(x,y)| \quad (10)$$

Perform additive convolution with high frequency component as follows

$$E_{LH}(x,y) = d(x,y) \oplus LH(x,y) \quad (11)$$
$$E_{HL}(x,y) = d(x,y) \oplus HL(x,y) \quad (12)$$
$$E_{HH}(x,y) = d(x,y) \oplus HH(x,y) \quad (13)$$

end for
return E_{LH}, E_{HL}, E_{HH}
end function

Function: Contrast Enhancement Phase

Input: Noise removed image with low resolution and poor contrast (I_{in})

Output: Enhanced high frequency sub-bands (E_{LH}, E_{HL}, E_{HH})

function *CEP* (I_{in})

- Function to enhance approximation coefficient sub-band

Read the image matrix I_{in}

for all points in I_{in} do

Compute Generalized Histogram Equalization (GHE)[36] for the input image 'I_{in}'

Compute LL, LL_1 sub-bands from GHE and input images using DWT as follows

$$LL(x,y) = \phi(x)\phi(y) \quad (14)$$

$$LL_1(x,y) = \phi_1(x)\phi_1(y) \quad (15)$$

end for

for each point in LL and LL_1 sub-bands do

Compute U, V *and* Σ components from LL sub-band using SVD as follows

$$U = \sigma^{-1}(LL)v \quad (16)$$

$$V = orthonormal(eigenvectors\ of\ (LL)^T(LL)) \quad (17)$$

$$\Sigma = \sqrt{(LL)^T LL} = \begin{pmatrix} \sigma^1 & & \\ & \ddots & \\ & & \sigma^n \end{pmatrix} \quad (18)$$

where v, σ, n are the eigen vector, eigen value and total number of eigen value of LL sub-band

Compute U_1, V_1 *and* Σ_1 from LL_1 sub-band as given in Eqs.(16) to (18)

end for

Calculate correction factor 'ξ', enhanced singular value matrix 'Σ_L' and LL sub-band of SVD 'LL_{SVD}' as given in Eqs. (19) to (21)

$$\xi = \frac{max(U)+max(V)}{max(U_1)+max(V_1)} \quad (19)$$

$$\Sigma_L = \xi x \Sigma_1 \quad (20)$$

$$LL_{SVD} = U x \Sigma_L x V^T \quad (21)$$

return LL_{SVD}

end function

Function: Reconstruction of Enhancement Image Phase

Input: LL_{SVD}, (E_{LH}, E_{HL}, E_{HH}) from *CEP* (I_{in}) and *REP*(I_{in}) respectively

Output: Enhanced image (E_{out})

function *RCEIP* (LL_{SVD}, E_{LH}, E_{HL}, E_{HH})

- Function to reconstruct the enhanced image

Read LL_{SVD}, E_{LH}, E_{HL} *and* E_{HH}

for each points in each enhanced sub-bands do

Reconstruct the enhanced image from LL_{SVD}, E_{LH}, E_{HL} and E_{HH} using IDWT

$$E_{out} = IDWT\ (LL_{SVD}(x,y) + E_{LH}\ (x,y) + E_{HL}\ (x,y) + E_{HH}(x,y)) \quad (22)$$

end for

return E_{out}

end function

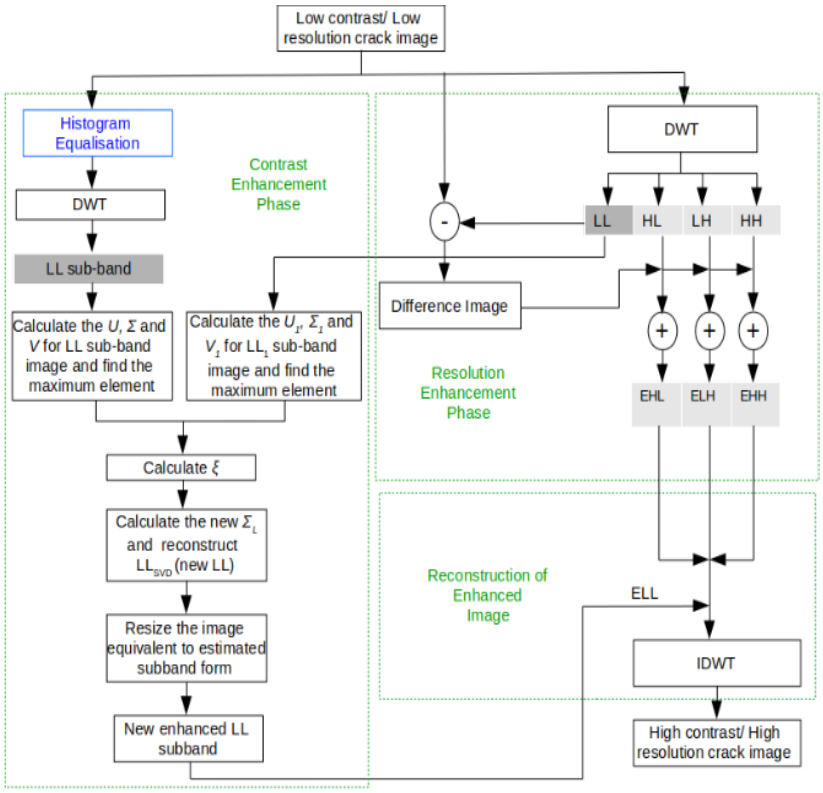

Figure 2. Proposed Hybrid Image Enhancement approach

3.1.3 Crack segmentation and connection - Morphological operations and KD Tree:

Crack regions are segmented from the enhanced image using appropriate morphological operations. In this method, adjacent pixels are connected using a closing operation. Also, the discontinuities in the crack segments are reconnected to a limited extent by filling in the smaller segments using K-Dimensional Tree (KD Tree) explained in Algorithm 3.

3.2. Feature Extraction and Crack Classification

In this stage, features are extracted from the segmented region with cracks, which are classified into specific types, based on their image features. In all, two statistical and six geometric features are retrieved. The two statistical features namely L_row (number of crack target intersecting with horizontal lines) and L_col (number of crack targets intersecting with vertical lines). The six geometric features are area, rectangularity, aspect ratio, eccentricity ratio, height and width. Neural network (MLP), kernel (SVM) and tree based approaches (AdaBoost, random forest and decision tree) are used to classify crack images from the extracted features into binary (crack vs non-crack) or multiclass regular, irregular and non–crack types [2, 4, 28].

Algorithm: KD Tree

Input: Enhanced image with discontinuities in crack region (I_{in})
Output: Enhanced image with connected crack region (C_{out})
procedure *KD Tree* (I_{in})

- Procedure to connect the discontinuities in the crack region
- Z, the number of samples

for k ⟶ 1 to Z do
  Read the image matrix I_k
  for i ⟶ 1 to M do
    for j ⟶ 1 to N do
      Compute endpoints $S = P_1, P_2, \ldots\ldots, P_d$ based on change in the intensity value

$$Standard\ Deviation = \sqrt{Variance} \quad (23)$$

where variance (σ^2) and mean are computed from Eqs. 1-2

      for each endpoint in S
        Calculate the distance with the adjacent end points as follows

$$d_{i,j} = \begin{cases} dis(P_i, P_j), & if\ i \neq j \vee (P_i, P_j)\ not exist \in the\ same\ crack\ line \\ 0, & if\ i = j \vee (P_i, P_j)\ exist \in the\ same\ crack\ line \end{cases} \quad (24)$$

where P_i corresponds to (x_i, y_i) and P_j corresponds to (x_j, y_j)

where $dis(P_i, P_j) = \sqrt[2]{(x_j - x_i)^2 - (y_j - y_i)^2}$ (25)

      end for
      if $d_{i,j}$ > Critical $threshold$ and $d_{i,j} \neq 0$ and $d_{i,j}$ $is\ unvisited$:
        while $d_{i,j}$ <= 0 :
          Connect the crack segment pixel wise from P_i to P_j in I_k
          Decrement $d_{i,j}$
        end while
      end if
    end for
  end for
  C_{out} ⟶ I_k
end for
return C_{out}
end procedure

4. Experiments

The proposed algorithm for crack detection, and classification with validation, are implemented in Matlab R2018b and Python 3.3.2, respectively, for the three datasets used. In this section, the description of the datasets, experimental results, and a performance evaluation with appropriate comparisons are explained.

4.1. The Dataset

For ease of explanation, existing datasets are named dataset 1 [26], dataset 2 [23] and the dataset acquired is dataset 3, described in Table 1, identifying the type of crack as well as the number of training and test images. Dataset 3 is a collection of images from DIGITLab, incorporating web and crack images acquired using a mobile camera on different concrete surfaces. Dataset 1 contains 40000 (20000 crack and 20000 non-crack) images with mostly prominent crack regions, captured using a low cost sensor. Dataset 2

contains 1018 (788 crack and 230 non-crack) low resolution, low contrast and/or shadowy images collected from different surfaces. Dataset 3 has 431 concrete (328 crack and 103 non-crack) low resolution, low contrast images. The dataset includes regular (longitudinal, transverse, thin, line-like, medium and large) and irregular (miscellaneous, crocodile, reflexive and complex) cracks.

Table 1. Dataset Description

Dataset		Crack Type	Training Set (No. of images)	Test Set (No. of images)	Total Images
Dataset 1 [26]		Crack	16000	4000	20000
		Non-crack	16000	4000	20000
		Total	32000	8000	40000
Dataset 2 [23]		Crack	477	311	788
		Non-crack	145	85	230
		Total	788	230	1018
Dataset 3 (Collected dataset)	Binary class	Crack	253	75	328
		Non-crack	83	20	103
		Total	336	95	431
	Multi - class	Regular Crack	124	36	160
		Irregular crack	129	39	168
		Non-crack	83	20	103

4.2. Experimental Results

The stage wise output obtained for the input image is illustrates in Figure 3, with WF, WE and WoE standing for the Wiener Filter, With Enhancement and Without Enhancement. It is evident that the input image without the HIE retains noise, unlike the crack region that is clearly segmented and classified with the HIE.

Further, the information on the enhanced crack images is analyzed with the original image using the metrics of entropy and standard deviation. It is inferred from the results that the entropy and standard deviation increased by 7.6% and 24.92%, respectively, for the enhanced images depicted in Table 2. In addition, noise levels are reduced and the appropriate feature values extracted.

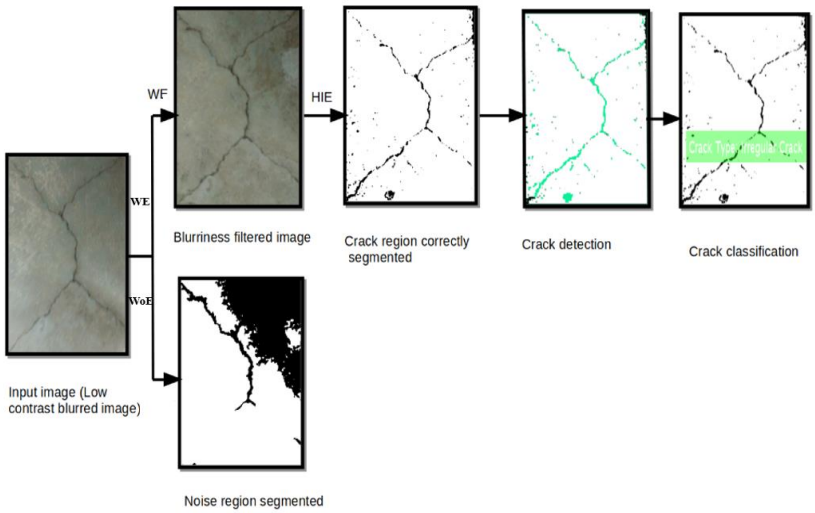

Figure 3. Result of Proposed System at Every Stage

Table 2. Performance of the HIE using Entropy and Standard Deviation

Concrete Crack Image	Entropy	Standard Deviation
Original image	5.8145	16.6888
Enhanced image	6.7631	27.7702

The KD Tree algorithm is used to connect the discontinuities in the crack region, following image enhancement and a morphological operation, as shown in Figure 4. Each connected component in the crack region represents the crack line, and the K-Nearest Neighbor (KNN) is used to distinguish the endpoint of each crack line, shown in different colors. Finally, based on the minimum distance value, the crack regions are connected and depicted in red.

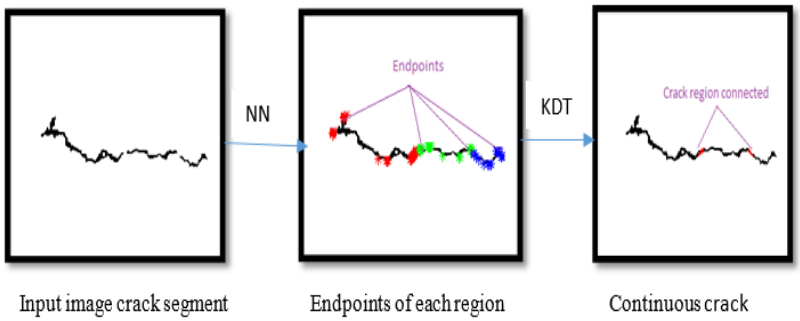

Figure 4. Result of KD Tree

4.3. Performance Analysis

From the segmented crack region, eight features (described in Section 3) are extracted and classified using the random forest, MLP, AdaBoost, SVM and decision tree algorithms. The classification results are analysed, performance-wise, for the three datasets (described in Table 1) using the metrics of accuracy, recall and precision. The results of the binary (crack vs. non-crack) and multiclass (regular, irregular and non-crack) classification are shown as graphs in Figure 5 and Figure 6, wherein each dataset with the HIE and Without Enhancement (WoE) is depicted in green and orange, respectively, and the State-of-the-Art (SoA) dataset in brown. The graphs shown are generated using Tableau Software. The scale used in the graph ranges from 0.0 to 1.0, with a step size of 0.1.

Figure 5. Graphical representation of accuracy Vs. datasets and methods for binary classification

The inferences obtained from an analysis of the features and the five classification algorithms versus the datasets (1, 2 and 3) for the HIE and WoE are listed below:

(i) From the extracted features, L_row and L_col plays an efficient role in computing characteristic difference between similar cracks at pixel level.

(ii) Dataset 1 resulted in 12% and 7% higher accuracy than dataset 2 and dataset 3, respectively, for the HIE, given that the prominence of the crack regions in dataset 1 resulted in better classification accuracy. (iii) As far as dataset 3 is concerned, binary class classification outperformed multiclass classification. In both cases, however, enhanced images outperformed than without enhanced images, as shown in Figure 5 and Figure 6.

(iv) In terms of classifiers, the random forest and AdaBoost algorithms are best suited to the classification of crack types, irrespective of the datasets (Figure 5 and Figure 6).

(v) A Comparative analysis with existing work: The proposed algorithm performed better for dataset 1 using the random forest rather than the CNN model (SOA) [23], because more significant and relevant features could be extracted. The metrics of accuracy, precision and recall are used for comparison, resulted with the improved values of 7%, 9% and 4%, respectively. For multiclass classification, the SOA [25] model resulted in a success rate of 80%, whereas the proposed model with enhanced images achieved 6% more accuracy for dataset 3 because it incorporated the HIE approach, resulting in an improved performance overall.

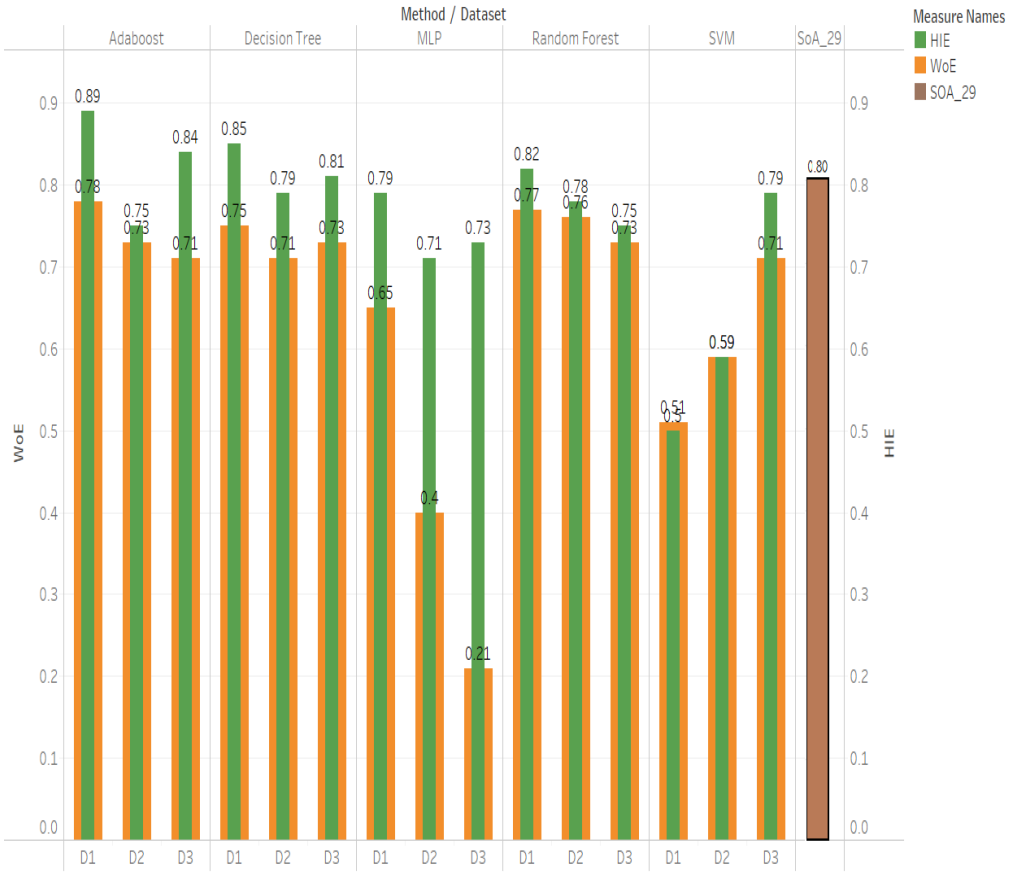

Figure 6. Graphical representation of accuracy Vs. datasets and methods for multiclass classification

Table 3 depicts a performance analysis of Datasets Vs Methods for the quantitative metrics of accuracy, precision and recall. Table 3 makes it clear that the proposed HIE algorithm has improved the performance overall, irrespective of the dataset and classification model used. With respect to five types of classification models considered, the random forest has the highest accuracy for enhanced and the AdaBoost for without enhanced crack images, even though the overall performance is less.

Table 3. Performance Analysis (Datasets Vs Methods)

Dataset		Accuracy	Precision	Recall	Method(s)
Dataset 1	WoE	0.86	0.86	0.86	AdaBoost and Random forest
	HIE	0.96	0.96	0.96	Random forest
Dataset 2	WoE	0.79	0.81	0.80	AdaBoost
	HIE	0.84	0.85	0.84	Random forest
Dataset 3	WoE	0.79	0.78	0.79	Support Vector Machine
	HIE	0.89	0.92	0.91	AdaBoost
SOA		0.89	0.87	0.92	Convolutional Neural Network

5. Conclusion and Future Work

This research has proposed an automatic crack detection and classification scheme to deal with cracks on concrete surface images, and the results obtained were compared with State-of-the-Art methods and datasets. The objective of the research was three-fold:

to classify low resolution or low contrast images into specific types, eliminate discontinuities in the crack region during segmentation, and apply a suitable classification algorithm for crack classification. The stages of the proposed system included preprocessing, image enhancement, segmentation of the crack region and classification of cracks into appropriate types. Preprocessing using the Wiener filter eliminated blurriness in the crack images. Low contrast and low resolution images were improved using the proposed HIE technique. Further, the crack regions were segmented by filling holes using morphological operations and the discontinuities connected using the KD Tree algorithm. Features extracted from the segmented crack region were classified into specific crack types using the random forest, MLP, AdaBoost, SVM and decision tree algorithms. The importance of the proposed HIE was analysed from the crack classification results for different datasets using the quantitative metrics of accuracy, precision and recall. Our findings revealed that the classification results for low contrast, low resolution and the blurred images shown a significant improvement with the HIE than without HIE. In addition, the results were computed and analysed for different datasets for binary and multiclass classification. The results of dataset 2 are more or less identical to those of the proposed dataset 3, because the images are low resolution, low contrast and/or shadowy in nature. Dataset 1 and 3 resulted in better classification accuracy for enhanced images in terms of both binary and multiclass classification, thus demonstrating the efficacy of the proposed HIE technique in civil infrastructure assessment.

The proposed work can be further improved for use in real time applications by maintaining a distance between the mobile camera and the location of the crack, capturing sustained high resolution images at specific time intervals through the use of UAVs or robots, and developing a single system that works to detect and classify all surface crack types.

Acknowledgments

We proffer our deepest gratitude to the Department of CSE, Sri Sivasubramaniya Nadar College of Engineering, for permitting us to utilize their High Performance Computing Laboratory to complete this research successfully. However, this research received no specific grant from any funding agency in the public, commercial, or not-for-profit sectors.

REFERENCES

[1] *H. Oliveira and P. L. Correia, "Identifying and Retrieving Distress Images from Road Pavement Surveys", IEEE International Conference on Image Processing, San Diego, USA,* ***(2008)*** *October 12-15. https://doi.org/10.1109/icip.2008.4711690*

[2] *Y. Chen, T. Mei, X. Wang and F. Li, F, "A Bridge Crack Image Detection and Classification Method based on Climbing Robot", Thirty fifth Chinese Control Conference, Chengdu, China,* ***(2016)*** *July 28-30. https://doi.org/10.1109/chicc.2016.7553984*

[3] *Y. S. Yang, C. M. Yang and C. W. Huang, C. W, "Thin Crack Observation in a Reinforced Concrete Bridge Pier Test using Image Processing and Analysis", Advances in Engineering Software, vol. 83,* ***(2015)****, pp. 99-108. https://doi.org/10.1016/j.advengsoft.2015.02.005*

[4] *M. Kamaliardakani, L. Sun and M. Ardakani, "Sealed-Crack Detection Algorithm using Heuristic Thresholding Approach", International Journal of Computing in Civil Engineering, vol. 30, no. 1,* ***(2016)****, pp. 1-10. https://doi.org/10.1061/(asce)cp.1943-5487.0000447*

[5] *P. Shi, X. Fan, J. Ni, Z. Khan and M. Li, "A Novel Underwater Dam Crack Detection and Classification Approach based on Sonar Images", Sarah and*

*George Journals, vol. 12, no. 6, **(2017)**, pp. 541-554. https://doi.org/10.1371/journal.pone.0179627*

[6] *W. Li, H. Ju, S. Tighe, Q. Ren and Z. Sun, "Three-Dimensional Pavement Crack Detection Algorithm based on Two-Dimensional Empirical Mode Decomposition", Journal of Transportation Engineering, vol. 143, no. 2, **(2017)**, pp. 1-12. https://doi.org/10.1061/jpeodx.0000006*

[7] *M. Salman, S. Mathavan, K. Kamal and M. Rahman, "Pavement Crack Detection using the Gabor Filter", International IEEE Conference on Intelligent Transportation Systems, Hague, Netherlands, **(2013)**, October 6-9. https://doi.org/10.1109/itsc.2013.6728529*

[8] *H. N. Nguyen, T. Y. Kam and P. Y. Cheng, "A Novel Automatic Concrete Surface Crack Identification using Isotropic Undecimated Wavelet Transform". IEEE International Symposium on Intelligent Signal Processing and Communication Systems, Tamsui, Taiwan, **(2012)**, December 3-6. https://doi.org/10.1109/ISPACS.2012.6473594*

[9] *X. Qiu, G. Li, J. Wei and C, "A Method of Crack Defects Real-time Image Enhancement in Continuous Casting Billet", Symposium on Photonics and Optoelectronics, Guilin, China, **(2012)**, October 29-31. https://doi.org/10.1109/sopo.2012.6270558*

[10] *R. Amhaz, S. Chambon, J. Idier and V. Baltazart, "Automatic Crack Detection on Two-Dimensional Pavement Images: An Algorithm based on Minimal Path Selection", IEEE Transactions on Intelligent Transportation Systems, vol. 17, no. 10, **(2016)**, pp. 2718-2729. https://doi.org/10.1109/TITS.2015.2477675*

[11] *X. Zhou, L. Xu and J. Wang, "Road Crack Edge Detection based on Wavelet Transform", Institute of Physics Publishing Conference series: Earth and Environmental Science, vol. 237, no. 3, **(2019)**, pp. 1-5. https://doi.org/10.1088/1755-1315/237/3/032132*

[12] *M. E. Torbaghan, W. Li, N. Metje, M. Burrow, D. Chapman and C. D. F. Rogers, "Automated Detection of Cracks in Roads using Ground Penetrating Radar", Journal of Applied Geophysics, vol. 179, **(2020)**, pp. 104-118. https://doi.org/10.1016/j.jappgeo.2020.104118*

[13] *N. Hoang, N, "Detection of Surface Crack in Building Structures using Image Processing Technique with an Improved Otsu Method for Image Thresholding", Advances in Civil Engineering, vol. 2018, **(2018)**, pp. 1-10. https://doi.org/10.1155/2018/3924120*

[14] *N. Sheerin Sitara, S. Kavitha and G. Raghuraman, "Review and Analysis of Crack Detection and Classification Techniques based on Crack Types", International Journal of Applied Engineering Research, vol. 13, no. 7, **(2018)**, pp. 6056-6062https://www.ripublication.com/ijaer18/ijaerv13n8_63.pdf*

[15] *F. Kallel and A. B. Hamida, "A New Adaptive Gamma Correction based Algorithm using DWT-SVD for Non-Contrast CT Image Enhancement", IEEE Transactions on Nanobioscience, vol. 16, no. 8, **(2017)**, pp. 666-675. https://doi.org/10.1109/tnb.2017.2771350*

[16] *M. Qiao, W. Xiaoying, W and Z. Yuan, "Research on a Least Squares Thresholding Algorithm for Pavement Crack Detection", Sixth International Conference on Information Science and Technology, London, UK, **(2016)**, July 26-28. https://doi.org/10.1109/icist.2016.7483459*

[17] *P. Wang and H. Huang, "Comparison Analysis on Present Image-based Crack Detection Methods in Concrete Structures", Third International Congress on Image and Signal Processing, Vancouver, Canada, **(2010)**, August 26-28. https://doi.org/10.1109/cisp.2010.5647496*

[18] *H. Liu, Z. Huang, Y. Zang and A. M. H. Ahmed, "Shape-based Micro Crack Detection in Plastic through Image Processing", International Journal of Signal Processing, Image Processing and Pattern Recognition, vol. 9, no. 1, **(2016)**, pp. 281-288. https://doi.org/10.14257/ijsip.2016.9.1.27*

[19] *L. Meng, Z. Wang and F. Y. Fujikawa, "Detecting Cracks on a Concrete Surface using Histogram of Oriented Gradients", International Conference on Advanced Mechatronic Systems, Beijing, China, **(2015)**, August 22-24. https://doi.org/10.1109/icamechs.2015.7287137*

[20] *P. Prasanna, K. J. Dana, N. Gucunski, B.B. Basily, H. M. La, R. S. Lim and H. Parvardeh, "Automated Crack Detection on Concrete Bridges", IEEE Transactions on Automation Science and Engineering, vol. 13, no. 2, **(2016)**, pp. 591-599. https://doi.org/10.1109/tase.2014.2354314*

[21] *W. Zhang, Z. Zhang, D. Qi and Y. Liu,. "Automatic Crack Detection and Classification Method for Subway Tunnel Safety Monitoring", Sensors, vol. 14, no. 10, **(2014)**, pp. 19307-19328. https://doi.org/10.3390/s141019307*

[22] *P. Chun, S. Izumi and T. Yamane, "Automatic Detection Method of Cracks from Concrete Surface Imagery using Two-Step Light Gradient Boosting Machine", Computer Aided Civil and Infrastructure Engineering, vol. 36, no. 1, **(2020)**, pp. 61-72. https://doi.org/10.1111/mice.12564*

[23] *M. Maguire, S. Dorafshan and R. J. Thomas," SDNET2018: An annotated Image Dataset for Non-Contact Concrete Crack Detection using Deep Convolutional Neural Networks", Data in Brief, vol. 21, **(2018)**, pp. 1664-1668. https://doi.org/10.1016/j.dib.2018.11.015*

[24] *H. Oliveira and P. L. Correia, "Automatic Road Crack Detection and Characterization", IEEE Transactions on Intelligent Transportation Systems, vol. 14, no. 1, **(2013)**, pp. 155-168. https://doi.org/10.1109/TITS.2012.2208630*

[25] *A. Cubero Fernandez, F. J. Rodriguez-Lozano, R. Villatoro, J. Olivares and J. M. Palomares, "Efficient Pavement Crack Detection and Classification", EURASIP Journal on Image and Video Processing, vol. 39, **(2017)**, pp. 1-11. https://doi.org/10.1186/s13640-017-0187-0*

[26] *N. M. Zaki, S. Deris, S and K. K. Chin, "Extending the Decomposition Algorithm for Support Vector Machines Training". Journal of Information and Communication Technology, vol. 1, no. 2, **(2002)**, pp. 17-29. http://e-journal.uum.edu.my/index.php/jict/article/view/7815*

[27] *N. Sheerin Sitara and S. Kavitha, "Comparative Analysis of Deep Neural Networks for Crack Image Classification", International Conference on Intelligent Data Communication Technologies and Internet of Things, Tamil Nadu, India **(2019)**, August 7-8. https://doi.org/10.1007/978-3-030-34080-3_49*

[28] *A. Mohan and S. Poobal, "Crack Detection using Image Processing: A Critical Review and Analysis", Alexandria Engineering Journal, vol. 57, no. 2, **(2018)**, pp. 787-798. https://doi.org/10.1016/j.aej.2017.01.020*